energies

MDPI

Article

Combined Wind Turbine Protection System

Vladimir Kaverin [1], Gulim Nurmaganbetova [2,*], Gennadiy Em [1], Sultanbek Issenov [2], Galina Tatkeyeva [2] and Aliya Maussymbayeva [1,*]

[1] Faculty of Energy, Automation, and Telecommunications, Abylkas Saginov Karaganda Technical University, 56 Nursultan Nazarbayev Ave., Karaganda 100027, Kazakhstan; kaverinkaverin@gmail.com (V.K.); gennadijem@gmail.com (G.E.)

[2] Energy Faculty, Saken Seifullin Kazakh Agrotechnical Research University, 62, Zhenis Ave., Astana 010000, Kazakhstan; issenov.sultanbek@gmail.com (S.I.); ttatkeeva@gmail.com (G.T.)

* Correspondence: sahitovna.1978@gmail.com (G.N.); maussymbayevaaliya@gmail.com (A.M.); Tel.: +7-701-537-7000 (A.M.)

Abstract: The increasing deployment of wind turbines in technologically advanced nations underscores the need to enhance their reliability, extend their operational lifespan, and minimize failures. The current protection devices for wind turbine components do not sufficiently shield them from various external factors that degrade performance. This study addresses the environmental and technical challenges that disrupt wind turbine operations and reviews existing research and technical solutions for protecting individual components, supported by experimental findings. Using a decomposition method followed by the integration of protection components, we propose a combined protection system designed to improve the overall resilience of wind turbines. The proposed system aims to reduce incidents, extend service life, and increase reliability, addressing a critical gap in wind energy technology and contributing to its continued development and efficiency.

Keywords: protection system; wind generator; wind turbine; emergency situations; icing; lightning; vibration; temperature increase

check for updates

Citation: Kaverin, V.; Nurmaganbetova, G.; Em, G.; Issenov, S.; Tatkeyeva, G.; Maussymbayeva, A. Combined Wind Turbine Protection System. *Energies* **2024**, *17*, 5074. https://doi.org/10.3390/en17205074

Academic Editor: Davide Astolfi

Received: 17 September 2024
Revised: 7 October 2024
Accepted: 9 October 2024
Published: 12 October 2024

Copyright: © 2024 by the authors. Licensee MDPI, Basel, Switzerland. This article is an open access article distributed under the terms and conditions of the Creative Commons Attribution (CC BY) license (https://creativecommons.org/licenses/by/4.0/).

1. Introduction

Despite the inherent instability of electricity produced by alternative energy sources, there has been a consistent increase in the amount of energy generated by these technologies. Currently, renewable energy accounts for 18% of the electricity consumed in the European Union, 20% in the USA, 28% in China, and 35.9% in Australia [1–5].

Alongside the deployment of new alternative energy sources, leading countries in this sector are focusing on reducing the environmental impact, enhancing the reliability of innovative technical solutions, and mitigating the influence of changing climatic conditions on these technologies [6–13].

The primary factors significantly influencing the development of wind energy include increasing the nominal power output; the specialization of wind turbine manufacturers in the production technologies of component parts; the growing trend of transitioning away from gearboxes towards direct-drive systems; and enhancing the competitiveness of wind turbines by reducing the cost of the energy they generate. This also involves the development of new materials and the optimization of the electromechanical components [14,15].

Reducing the cost of electricity generated by wind turbines can be achieved by minimizing the occurrence of emergency situations and extending the service life of wind turbines. One way to address this issue is through the investigation of emergency situations and the development of technical solutions for a combined protection system based on the obtained results.

There are also other methods to improve the efficiency of wind turbines, such as enhancing the aerodynamic design of the turbine structure. In the study [16], a two-dimensional unsteady computational fluid dynamics (CFD) analysis was conducted on an

inclined airfoil to assess dynamic stall and aerodynamic forces affecting the wind turbine structure. Aerodynamic forces, fluid flow structures, and flow separation delay angles were examined depending on the Reynolds number, reduced frequency, oscillation amplitude, and mean angle of attack.

The main advantages of wind turbines over other electricity generation methods include their lack of reliance on fuel resources or ash disposal, as required in coal-fired power plants. Therefore, there are no costs for building and maintaining ash storage facilities or reclaiming them later. Wind turbines also produce no emissions of carbon dioxide, sulfur, or ash. Unlike solar panels, they do not suffer from the degradation of semiconductor elements that convert solar energy into electricity.

Wind turbines with horizontal axes of rotation are the most widely used, including those produced by companies such as Siemens Gamesa (Hamburg, Germany), Vestas Wind Systems A/S (Aarhus, Denmark), and others [16,17].

This wind turbine model has the highest energy conversion efficiency, transforming wind energy into electrical energy. One of the operational characteristics of wind turbines with a horizontal axis of rotation is the increased vibrations, which span a wide frequency range. These vibrations negatively affect both the soil fauna surrounding the turbine's foundation and the surrounding airspace. The power equipment of a horizontal-axis wind turbine (Figure 1) includes the rotor (1) and the system for converting wind energy into electrical energy located in the nacelle (2) [18–20].



Figure 1. The horizontal-axis wind turbine.

For offshore wind turbines, the floating design with a vertical axis of rotation has become widespread. The company SeaTwirl (Stavanger, Norway) is developing such wind turbines, specifically the S2 model with a capacity of 1 MW. In the future, it is planned to increase the capacity of the wind turbine to 30 MW [8]. The design of the S2 model allows for efficient operation at wind speeds of up to 50 m/s. The appearance of the offshore wind farm is shown in Figure 2. A distinguishing feature of the proposed design is the high density of wind turbines placed on the water's surface [21,22].

Wind turbines can operate both in grid-connected mode, supplying electricity to the power network, and in standalone mode, where the wind turbine serves as the sole source of electrical energy for consumers. The technical characteristics of the generated energy are controlled through power semiconductor converters.



Figure 2. Offshore wind farm.

Analysis of Disruptive Factors in Wind Turbine Operation and Technical Solutions for Protecting Structural Elements:

Disruptive factors affecting wind turbine operation can be categorized into two groups: the first group is defined by climatic conditions, while the second is related to the technical state of the wind turbine's structural elements and power supply systems.

Climatic factors that significantly impact the reliability of wind turbines include:

- Wind speeds that significantly exceed the maximum allowable limits specified by the turbine's technical characteristics, variations in air flow acceleration, and its oscillation frequency;
- Lightning strikes, including their frequency, spatial alignment between the area of lightning strikes and the location of wind turbines, as well as the energy characteristics of the strikes;
- The icing of wind turbine components, including the intensity and duration of the icing.

Negative factors related to the technical condition of the wind turbine's electromechanical systems include:

- The wear and tear of mechanical components such as turbine bearings, gearboxes, generators, and mechanical braking systems;
- The degradation of the insulation properties of generator winding wires and electrical cables used in the wind turbine;
- The deterioration in the performance of the cooling systems for the electromechanical components of the wind turbine;
- The overheating of the wind turbine's electromechanical converter windings.

Researchers led by Nicholas T. Luchetti (Department of Atmospheric and Oceanic Sciences, University of Colorado) and Arrieta-Prieto M. (Wei Yiming Key Laboratory of Atmospheric Environment and Extreme Meteorology, State Key Laboratory of Atmospheric Boundary Layer Physics and Atmospheric Chemistry, Institute of Atmospheric Physics, Chinese Academy of Sciences) have studied the characteristics of the airflow at the boundaries of storm fronts in mountainous and flat terrain [23–26].

Storm fronts create localized loads on wind turbine structures that exceed the maximum permissible values. Previous studies have examined the impact of storm fronts in flat terrain [27].

This study presents the results of research on the effects of storm fronts in areas with complex terrain, including rocky mountains. Experimental findings revealed that in mountainous regions, the values of controlled parameters (wind speed, temperature, humidity, and turbulence at altitudes not lower than 300 m) are slightly lower compared to those during storms in flat regions. However, it is worth noting that the peak wind

turbulence kinetic energy reached 4 $m^2 \cdot kg \cdot s^{-2}$. The high dynamics of wind speed during a storm front reduces the reliability of mechanical components in wind turbine structures.

In flat terrain, static wind speed, changes in direction, and acceleration are significantly higher than in mountainous areas. In coastal regions, typhoons have a substantial negative impact on wind turbine structures. Wind speeds in the central area of a typhoon can reach 50 m/s, with gusts of up to 70 m/s, and the radius of storm winds can extend to 170 km [28,29].

In the United States, Europe, and Australia, tornado formation is highly probable. Wind speeds in the center of a tornado can reach 130 m/s, and the tornado's diameter can be as large as 3 km. A decrease in temperature is observed with the height of the cyclone. Tornadoes are often accompanied by lightning strikes, adding to the negative impact [30,31].

Exceeding the maximum permissible wind speed for wind turbines leads to increased vibration amplitude and the bending of the horizontal-axis wind turbine structure. Dynamic loads on the mechanical components of the wind turbine result in the development of micro-cracks in its metal elements and, in some cases, the destruction of the entire structure. By monitoring key parameters (wind speed, air temperature, vibration amplitude, and the angle of inclination relative to the horizon) and adjusting the operating modes of the wind turbine, it is possible to minimize the negative impact on the turbine's structure.

Researchers Ren Yushu, Xu Weixin, and Fu Jiaolan from Sun Yat-Sen University and Southern Marine Science and Engineering Guangdong Laboratory (Zhuhai, China) have conducted studies on lightning density and its correlation with climatic conditions in China [32].

The likelihood of a lightning strike hitting a rotating wind turbine is significantly higher than for a stationary one. To reduce the risk of lightning strikes during storm fronts in wind farm areas, it is recommended to stop the turbines from rotating.

In previous experimental studies, a correlation between the increase in lightning strikes and warming was established. During the evaluation of the energy characteristics of lightning, it was determined that the duration of a lightning strike does not exceed 2 s, and the current of the lightning leader can vary from 10 to 500 kA, with the average energy of a single lightning strike reaching up to 500 MJ. With such energy characteristics, a lightning strike on a wind turbine structure would likely cause a fire [33].

A group of specialists from Pakistan, China, and the USA, led by Ain Noor Ul from the Department of Electrical Engineering at the University of Engineering and Technology (Pakistan), has proposed a software solution for detecting lightning strikes based on fuzzy logic. Experimentally obtained data were used to verify the accuracy of the software, achieving a prediction probability of 98% [34].

Currently, lightning activity is predicted indirectly using specialized software (https://www.ecmwf.int (accessed on 8 October 2024)). The main informational parameters for predicting the onset of lightning and the frequency of strikes include changes in air temperature, the temperature at the lower edge of clouds, and the speed of vertical air currents. The combination of the velocity and acceleration of these variables indicates the likelihood of thunderstorm cloud formation and, consequently, lightning strikes. Experimental research has established a link between lightning activity and solar activity. Solar activity significantly influences the intensity and energy characteristics of lightning. It has been observed that two days after a solar flare, the electric field strength in thunderstorm clouds increases by 60%. Over the following two days, a gradual decrease in electric field intensity is noted. When solar wind reaches Earth's atmosphere, it increases atmospheric ionization, which in turn raises lightning activity. The duration of lightning activity roughly corresponds to the duration of the solar flare [35–38].

In developing a wind turbine protection system, an important aspect is the detection and geolocation of lightning strikes. Lightning detection is typically implemented using acoustic and electromagnetic control indicator sensors. A distinguishing feature of these sensors is the delay in the sensor's response to a lightning leader. Acoustic sensors have

a significantly longer delay than electromagnetic sensors, which detect electromagnetic bursts [39,40].

At the New Mexico Institute of Mining and Technology, research has been conducted on a combined lightning detection sensor. This sensor consists of panoramic optical and acoustic sensors. The combination of these sensors allows for the highly accurate geolocation and assessment of the energy characteristics of lightning strikes. During experimental studies, the spectral characteristics of the acoustic sensor signal were determined, enabling a high probability of identifying lightning strikes between clouds and between clouds and the ground [37,41].

The use of a combination of acoustic and optical sensors allows for determining the distance to a lightning strike by measuring the delay between the acoustic sensor's response and the optical sensor's response. By analyzing the change in distance to the lightning strike over time, it is possible to assess the approach of a storm front towards the monitored object.

A lightning strike forms a conductive channel of cold plasma through which an impulsive current flows, with peak values reaching several tens of thousands of amperes. A lightning strike is accompanied by a broad spectrum and high intensity of the electromagnetic field. Theoretical studies conducted at Khaldoun University (Algeria) have investigated the attenuation of the electromagnetic field generated by a lightning strike in space. The study presents findings on the effect of the electromagnetic field on the reliability of electronic control system units [42].

Based on the results of this research [42], it can be hypothesized that lightning strikes can be detected through the bursts of electromagnetic fields they generate.

Wind turbines have a complex mechanical structure, with each component serving a specific function. Climatic conditions, particularly low ambient temperatures, have a significant negative impact on wind turbine performance. One such negative climatic factor is the icing of the mechanical components of the turbine.

The accumulation of ice on the mechanical parts increases both static and dynamic loads on the entire wind turbine structure. Icing causes turbine imbalance, increases the amplitude of vibrations throughout the structure, and consequently raises the likelihood of component failure, reduces profitability, and shortens service life. The rate of ice formation largely depends on humidity, ambient temperature, and the duration during which environmental conditions around the turbine are conducive to ice formation. Uneven ice buildup on turbine blades leads to imbalance, increasing vibration amplitude and reducing energy output at the same wind speed.

One technical solution for managing icing is the development of icing detectors. This field has seen significant theoretical research and the development of devices and algorithms for wind turbine control systems. Considerable attention is being paid to the development of automated systems that detect the onset of icing, particularly in unmanned aviation and wind energy. In unmanned aviation, icing on aircraft structures typically leads to crashes and subsequent destruction. Therefore, in unmanned aviation, it is crucial not to predict icing but to detect its onset with minimal delay, allowing the flight path to be adjusted to avoid areas with a high risk of icing.

In the development of algorithms for determining the onset of icing, graph theory methods, as well as structural and parametric optimization techniques, are used [43,44].

Wind turbines do not have the ability to avoid icing. The primary task for wind turbines is to organize a sequence of measures that minimize the negative impact of icing, followed by a return to normal operating conditions after the icing has subsided. The key objectives in minimizing the negative impact include forecasting the onset of icing, developing a plan of action to reduce the negative effects of icing, and determining the appropriate time to resume normal operation [45–48].

To improve the accuracy of forecasting the onset of icing on wind turbine structures, it is proposed to use a variable polling rate for information sensors and to calculate the probability of icing. The development of an icing onset observer was implemented using

graph theory for the structural and parametric adaptation of the observer. Experimental studies were conducted on several wind turbines, resulting in a high level of accuracy in predicting the timing of icing on turbine components. It is worth noting that reducing the polling interval of the sensors, combined with calculating a parameter that characterizes the intensity of icing as a function of the probability of icing onset, significantly improves prediction accuracy.

A team of specialists led by Li Qingying (School of Air Transportation, Shanghai University of Engineering Science, China) proposed a method for detecting icing using infrared technology. By utilizing previously obtained data on ice thickness, a correlation function was constructed, enabling the prediction of icing development [49,50]. However, during the implementation of this forecasting method, it is necessary to consider the possibility of ice formation on the optics of the thermal imager.

At Western Petroleum University (China), research was conducted on predicting the intensity of icing. During theoretical studies, spatial approximation methods were used to model the growth in ice thickness and the increase in its surface area using the Fourier series, as well as taking into account the geometric characteristics of symmetrical profiles of rotor components in wind turbines (Figure 1). The prediction error did not exceed 10% [51].

It should be noted that using extrapolation methods in observers while increasing the time interval between sensor readings reduces the dynamic accuracy of the prediction process.

Icing on wind turbine components leads to a decrease in the power generated by the turbine at the same wind speed. This fact forms the basis for developing a system to monitor and predict the intensity of icing. To improve prediction accuracy, a three-level model is proposed. The first level uses an analytical system that models the dependence of icing intensity on generated power and wind speed; the second level introduces a correction for modeling errors. On the third level, fuzzy logic-based algorithms are applied to assess the reduction in the reliability of the wind turbine depending on the degree of icing [52,53].

This method of monitoring icing intensity allows for tracking the development of ongoing icing but does not enable the prediction of its onset.

Another factor with a significant negative impact is the occurrence of fires in wind turbines. When a fire starts, the turbine usually burns completely. The main causes of fires in wind turbines include the following:

- The heating of transmission oil, leading to changes in its structure due to thermal aging and subsequent mass loss;
- The degradation of the insulation properties of electrical cables;
- The use of certain polymer materials in the mechanical components of wind turbines;
- Lightning strikes hitting the wind turbine structure;
- The degradation of the insulation properties of electromechanical converter windings;
- The slippage of braking device surfaces during turbine shutdown;
- Insulation breakdown in high-voltage equipment due to switching overvoltages.

Wind turbine gearboxes, which function to couple the turbine's rotational speed with the energy converter, use transmission oil. Significant seasonal temperature fluctuations, high daily temperature changes, and heating from direct sunlight accelerate the thermal aging of transmission oil. As the oil thermally ages, its lubricating properties degrade, increasing friction in the gearbox, which in turn raises the oil's temperature. The rate of thermal aging is highest in the first week, but it slows over time. Research has shown that the thermal aging of transmission oil can lead to wind turbine fires [51,54].

Disruptive factors with a high likelihood of causing fires include bearing and gear wear. A monitoring method based on the spectral characteristics of vibrations in the mechanical components of wind turbines is proposed. The technical aspect of this diagnosis is based on the three-coordinate monitoring of the amplitude-frequency characteristics of vibration signals from three-axis sensors. Using a fast Fourier transform, the spectral characteristics of the vibration signal were obtained along three axes. This method can identify faulty components in the wind turbine's mechanical system, thereby preventing fires [55].

The capabilities of this method can be significantly expanded by incorporating elements of fuzzy logic to identify the component with deviations and assess its wear. The next stage could involve predicting the degree of wear on transmission components using extrapolation methods. This would allow for the timely replacement of worn components before an emergency situation arises.

During experimental research, the comparative characteristics of two types of braking systems were identified: one with sintered active layers containing fibrous and powdered metal additives in the brake pads and the other with pads made of ceramic composite materials. One of the negative aspects of brake pads with sintered active layers is the occurrence of sparks at the interface between the brake pad and the metal pulley during braking, which can lead to a fire in the turbine nacelle. To prevent fires, the wind turbine manufacturer equipped the braking system with an automated fire suppression system. Another approach to reducing the likelihood of fires during emergency braking is the development of a braking system using ceramic composite materials [56].

In the course of investigating the causes of wind turbine fires, experts from Long Yuan (Beijing) identified factors that increase the likelihood of fires. One factor contributing to fires is the occurrence of switching overvoltages in the power circuit of wind turbine electrical equipment.

In the Jilin province, a wind turbine's power transformer caught fire. During the switching of the power circuit, the resulting overvoltages led to rapid insulation degradation in the transformer windings, which can cause an electrical arc explosion. These switching overvoltages caused the transformer, located in the power converter cabinet at the base of the turbine, to catch fire, resulting in severe damage to the wind turbine [57].

A team led by Xuezhong Liu (State Key Laboratory of Electrical Insulation and Power Equipment, Xi'An Jiaotong University) proposed a method for assessing the condition of electrical insulation in wind turbine equipment. The proposed method is based on the accelerated aging of the insulation materials used in megawatt-class wind turbine power equipment. During testing, the following parameters were varied: repetitive pulse voltage, sample temperature, ambient humidity, salt mist, and vibration. These factors were studied both individually and in combination. After testing, the breakdown voltage was measured, and the dielectric properties of the insulation materials were analyzed over time. As a result of the experimental research, two main methods for evaluating the properties of insulation materials were proposed, specifically for offshore wind turbines and those located far from the coast [58–60].

However, one of the limitations of these methods is that they cannot be used for the real-time monitoring of the condition of the insulation materials in wind turbine electrical equipment.

In [61], experimental studies on the aging of Luminol™ TRi transformer oil were conducted. The evaluation of the insulating properties of interlayer paper insulation impregnated with oil was performed by monitoring the breakdown of the paper–oil insulation. High-frequency high-voltage electricity was used for the breakdown. As a result of the experiments, the aging intensity was determined under different ambient temperatures.

To forecast fire-hazardous situations, a method was proposed based on controlling the temperature of energy-dense zones of wind turbines, considering the power they generate. This method involves managing the generated power to reduce the temperature of the monitored object, thus preventing or delaying the occurrence of a predicted accident [62].

The limitation of this method is its applicability only for predicting fire-hazardous emergency situations in the power components of wind turbine electrical equipment.

Negative disruptive factors for wind turbines operating in energy transmission mode include the following:

- Significant changes in electrical parameters and resonance phenomena in the power grid;
- Short circuits, conductor breakages, and lightning strikes on the conductor of overhead power transmission lines;
- The switching of reactive elements in the power line.

One of the key challenges in improving the efficiency of wind turbines during energy transmission to the grid is minimizing the time needed to restore turbines to their normal operating state.

To reduce the time required to return the power supply system to working condition after an emergency that leads to the shutdown of part of the grid, an adaptive automatic reclosure system has been proposed. The duration of the reclosure process is determined by monitoring the completion of transient processes in the affected section of the power line. Once this is confirmed, a command is issued to restore the functionality of the affected power line section [62].

However, the issue of controlling the duration of transient processes in the affected section of the power line remains unresolved.

The number of technical solutions for wind turbine designs is constantly growing. Not only are the designs of electromechanical converters and their control methods evolving, but so are the power components, control systems, and technical solutions for matching the electrical characteristics of the generator system with the external power grid.

A method for fault registration has been considered for localizing defects in the power components of generator installations, followed by automated decision-making. The proposed method is based on fault classification, and using identification methods, a fault database is created for the power components of generator installations.

Experimental research on the accuracy of fault detection using a three-phase power converter showed a detection accuracy of no less than 96.5% [63].

Even for a local wind turbine, the creation of a fault database for the power components of generator installations, followed by fault identification and automated decision-making, remains a relevant issue. The reliability and stability of wind turbines equipped with semiconductor inverters and operating in grid-connected electricity generation mode are significantly affected by their technical condition and electrical parameters.

An analysis was conducted on high-frequency resonance occurring in the power grid, which has its own inductive and capacitive components. The results of studies on the occurrence of high-frequency resonance in distributed networks of 35 and 110 kV are presented. Installing filters in the power circuit does not eliminate the occurrence of voltage resonance, which serves as an additional disruptive factor.

In addition to high-frequency resonance, the reliability of wind turbines is also impacted by low-frequency transient processes determined by the voltage and frequency regulation system of the inverter [64,65].

Currently, asynchronous generators and doubly-fed machines are widely used as electromechanical converters with capacities over 1 MW [66,67].

The use of these machines in wind turbines has enabled power extraction over a broader range of wind speeds. Wind turbines with capacities exceeding 1 MW generally operate in grid-connected mode, transmitting energy to the general power grid. In this case, the turbines are equipped with devices that match the electrical characteristics of the generator with those of the power grid. Changes in the technical characteristics of the general power grid have a significant impact on the reliability of wind turbines [68,69].

A team of specialists from the Engineering Department of the Egyptian Holding Company for Silo and Storage, Beni Suef, Egypt, led by Taha Ahmed Enany, conducted research on a method for determining the heating temperature of the windings in an asynchronous machine.

The method is based on the linear dependence of stator winding resistance on its temperature. This approach involves calculating the resistance of the stator winding temperature by applying a small DC voltage, in addition to the AC supply voltage, to one of the stator windings. The DC bias voltage is applied continuously throughout the operation. During operation, the magnitude of the DC current is monitored and used to calculate the resistance and temperature of the stator winding. Using an artificial neural network based on a Takagi–Sugeno fuzzy inference system (ANFIS), accurate temperature values for the stator winding were obtained. The adequacy of this method was evaluated

through experimental studies by comparing the results with temperatures measured using a Perfect sensor. Experimental verification was conducted on a 7.4 kW asynchronous machine under different load conditions. This method proved effective for asynchronous machines with power ratings up to 10 kW [70].

However, one of the drawbacks of this method is the potential for the saturation of the magnetic core of the asynchronous machine. As the power of the motor increases, the power of the DC bias source must also increase, which could lead to magnetic core saturation and the deterioration of the thermal characteristics. Additionally, as the power of the asynchronous machine increases, the energy consumption for maintaining the calibrated DC bias voltage also rises.

Xi'an Huaao, a specialist from Xian Huaao Electronic Technology Co. Ltd. (Quzhou, China), highlighted the importance of developing protection devices for asynchronous machines to prevent overheating. The temperature of an asynchronous machine depends on the ambient temperature, the speed and direction of the airflow near the machine, as well as its operating mode and duration of use. The patent authors proposed a relay protection device for motor overheating based on the effect of changing the geometry of a bimetallic strip in response to the temperature of a heating element, which is connected to the stator winding power circuit of the motor [71].

One drawback of this device is that the maximum allowable temperature of the stator windings depends on the insulation class and cooling system. The current temperature of the stator windings is influenced by the ambient temperature and the speed and direction of the airflow near the asynchronous machine. If the motor operates outdoors, the temperature of the stator windings will also depend on climatic conditions.

A group of specialists led by Mortimer W. Fish proposed a technical device to protect the motor from overheating of its windings [72]. This device is based on the use of a temperature-sensitive resistor. The temperature-sensitive element must have a negative temperature coefficient of resistance. A drawback of this device is the need to modify the motor's design to ensure heat exchange between the temperature-sensitive resistor and the components of the electrical machine.

2. Materials and Methods

In preparing this manuscript, ChatGPT-4o, an AI language model developed by OpenAI, was used solely to assist with language editing and improving the clarity of the English text. It was not involved in generating, analyzing, or interpreting any scientific data or content related to the research.

The analysis of emergency situations in wind turbines and the technical solutions that implement protection and forecasting devices was carried out separately for each natural phenomenon (icing, lightning strikes on the turbine, wind gusts exceeding the maximum allowable speed for the turbine) and the technical condition of wind turbine components.

The method of decomposition and subsequent integration of the components of the combined system used in this study allows us to assert, through the use of previously completed research and developed technical solutions confirmed by experimental results, that the combined protection system for wind turbines being developed will ensure the real effectiveness of the applied methods and technical solutions. This decomposition was carried out to divide the comprehensive combined system into separate components, the technical solutions for which had been previously studied using simulation modeling and tested with hardware tools [23–72].

One of the tasks in improving the technical reliability of wind turbines is the development of a combined protection system for the electromechanical equipment of wind turbines [73,74].

In the study [75], the issues of the impact of dynamic wind characteristics and other climatic factors on the reliability of wind turbine operation are examined. The theoretical foundations for designing rotor components are presented, and methods for developing wind turbine control systems are discussed. The necessity of a combined protection system

is justified. The materials from the study helped identify the set of climatic factors and structural features of wind turbines that significantly affect their reliability.

The combined protection systems proposed in [75] are multi-level systems. The lowest level involves real-time monitoring of the technical condition parameters of wind turbine electromechanical equipment. This level is technically implemented using independent hardware devices—direct measurement sensors equipped with their own controller for processing and storing real-time information.

The second level includes observers that continuously calculate missing coordinates that cannot be monitored by direct measurement sensors. These observers use indirect methods to estimate the system's coordinates. The second level is typically implemented with modular controllers.

At the third level, the control signal is calculated based on the signals from the first and second levels, which provide information on the technical state of the electromechanical equipment and its derivatives.

The derivative is introduced into the combined protection system to assess the intensity of change in the monitored parameter [75].

In [76], an original method for calculating the derivative is proposed using a nonlinear approach based on the delay time of the monitored signal's coordinate. A new method for estimating the derivative through redefinition of the delay matrix is also presented. This method has been tested for calculating the derivatives of both clean and noisy signals. The research demonstrated that the derivative was calculated with sufficient accuracy. This is particularly relevant for wind turbines with semiconductor inverters, where signal noise can be a significant issue.

The fourth level of the combined protection system handles the generation of a set of control signals. This software block is also implemented within the control controller.

The proposed protection system will help reduce operational costs and extend the lifespan of wind turbines, thereby lowering the cost of electricity generation.

Disruptive factors that reduce the reliability of the electromechanical components can be divided into two main groups. The first group includes factors related to natural phenomena, while the second group pertains to the technical condition of the electromechanical equipment and peripherals of the wind turbine, including the electrical parameters of the power grid when operating in grid-connected mode.

In designing the combined protection system, the key tasks are the following:

- Classification of disruptive factors, identification of controllable coordinates for each factor, and determination of control actions;
- Assessment of the impact and economic damage caused by disruptive factors;
- Classification of control actions that prevent failure of wind turbine components.

One of the critical tasks in improving technical reliability is the research and development of a combined protection system for the electromechanical equipment of wind turbines [76].

Requirements for the Combined Protection System:

Based on the previous analysis of existing technical solutions for wind turbine designs, the cause-and-effect relationships between natural phenomena and emergency situations, operational performance violations, and safety issues during scheduled maintenance, a comprehensive set of technical requirements has been developed for the combined protection system.

The combined wind turbine protection system should ensure the following:

- Real-time monitoring of approaching storm fronts;
- Calculation of probability and detection of icing onset;
- Continuous monitoring of wind speed;
- Real-time monitoring of the temperature of transformer windings, gearbox, mechanical brake, and generator windings;
- Real-time monitoring of the wear condition of turbine bearings, generator bearings, gearbox bearings and gears, and the mechanical brake;

- Calculation of the remaining service life of wind turbine structural components;
- Automatic generation of recommendations for the operator and control commands in pre- and post-emergency situations;
- Supervisory control and management with process visualization.

The implementation of the combined protection system will ensure the following:

- Reduction in the likelihood of fire in the wind turbine;
- Prevention of emergency situations due to icing of wind turbine components;
- Reduction of structural loads when wind speeds exceed maximum permissible values;
- Minimization of the impact of lightning strikes on the turbine's mechanical components and control systems;
- Reduction of emergency situations due to wear on wind turbine bearings, generator bearings, gearbox bearings and gears, and the mechanical brake;
- Maximized utilization of the service life of controlled mechanical components of the wind turbine.

Structural Diagram of the Combined Protection System:

To implement the full range of technical requirements for the combined protection system, a three-level hardware structure is necessary (see Figure 3).

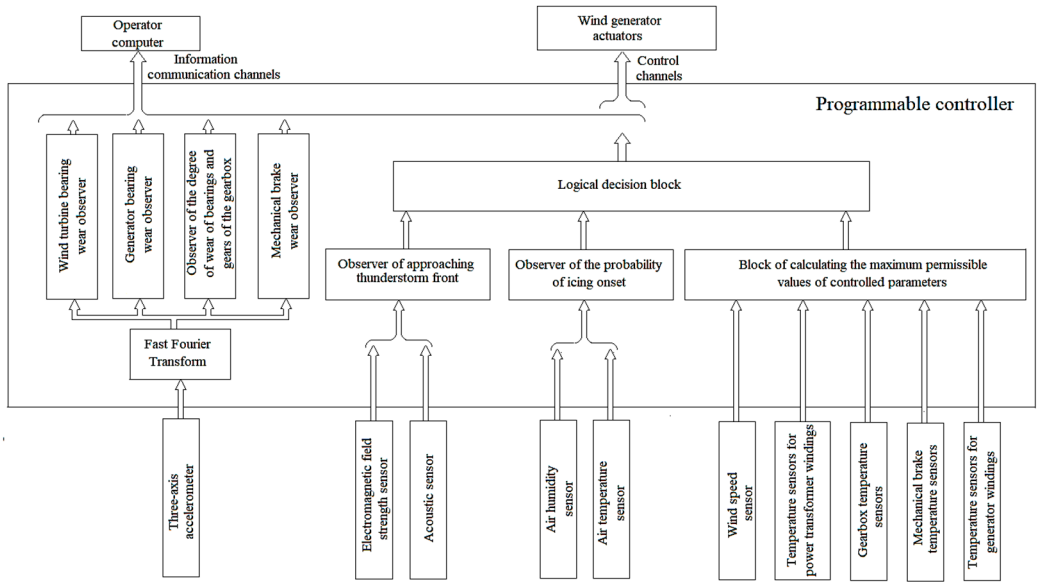


Figure 3. Structural diagram of the combined wind turbine protection system.

The first (lower) level consists of a set of control and indication sensors. This level is responsible for real-time data collection on the technical condition of the wind turbine. The indication sensors transmit information to the second level (controller) via communication channels. The control and indication sensors can be divided into two groups based on the monitored parameters.

The first group of sensors monitors the technical condition of the mechanical components of the wind turbine, including the turbine bearings, gearbox, generator, and mechanical brake. The second group of sensors monitors the environmental impact on the wind turbine, such as icing, exceeding the maximum allowable wind speed, and the approach of a storm front. Humidity and air temperature sensor data serve as input parameters for the observer to calculate the probability of icing onset and the duration of icing on the turbine's components. The electromagnetic field intensity sensor and acoustic sensor detect the approach of a storm front. The wind speed sensor determines the current wind speed. The collected information is transmitted to the second level [77].

At the second level, using observer algorithms, it is necessary to do the following:

Determine numerical values for coordinates that cannot be monitored by control and indication sensors;

Calculate the maximum allowable wind speed and the temperature limits for the transformer windings, gearbox, mechanical brake, and generator windings.

If the current calculated values exceed the defined maximum allowable limits, information about the approaching storm front and the probability of icing onset should be sent to the decision-making logic block.

The decision-making logic block will generate control commands for the wind turbine, aimed at reducing the negative impact of the aforementioned factors.

The real-time data from a three-axis accelerometer, along with the operation of the observer monitoring the wear of wind turbine bearings, generator bearings, and gearbox bearings and gears, form the basis for calculating the current values of the remaining service life for these components.

The second level of the combined protection system is implemented via a programmable controller. The main functions of the controller are the following:

Calculating control parameters through observers;

Generating control commands during relevant emergency situations;

Providing recommendations for the wind turbine maintenance personnel, as outlined in Table 1.

Table 1. Main functions of the combined protection system in emergency situations.

No.	Emergency Situation	A Set of Commands for a Combined Protection System
1	Reducing the calculated residual life of wind turbine bearings, generator bearings, gearbox bearings and gears and mechanical brakes.	Generation of the appropriate information message to the wind turbine operator.
2	Storm front approaching	1. Rotor shutdown. 2. Powering down of electrical and informational devices. 3. Blocking of input circuits for informational channels. 4. Generation of an information message to the wind turbine operator.
3	Icing onset	1. Rotor stop. 2. Generation of an information message to the operator regarding the start of icing and the turbine shutdown.
4	Exceeding the maximum permissible wind speed	1. Feathering of the wind turbine blades. 2. Stopping the rotor. 3. Generating an information message for the wind turbine operator.
5	Exceeding the permissible temperature of the power transformer windings, generator windings, gearbox, mechanical brake.	1. Rotor shutdown. 2. Disconnection of power devices from the external power source. 3. Generation of the appropriate information message to the wind turbine operator.

The third level of the combined protection system consists of an operator's computer equipped with software for visualizing technological processes (SCADA). The operator's computer should display real-time data on wind speed, the temperature of monitored wind turbine components, and the remaining service life of the turbine, gearbox, generator, and mechanical braking system, along with recommendations for maintenance personnel and commands generated by the decision-making logic block.

The dynamics of parameters such as the approach of a storm front, icing onset, wind speed exceeding the maximum allowable limit, and the temperature of the transformer windings, generator windings, gearbox, and mechanical brake are very rapid, and emergency situations can result in significant economic losses. Therefore, it is essential to make quick decisions to mitigate the consequences of these emergencies [75].

Based on the previously developed functional diagram (Figure 3) and the list of main controller functions (Table 1), the controller algorithm for the combined protection system has been developed (Figure 4). The primary purpose of the combined protection system

is to notify the operator about potential or actual emergency situations, execute turbine shutdown operations, generate recommendations for the operator on how to address the emergencies, and issue a command to initiate the turbine shutdown procedure.

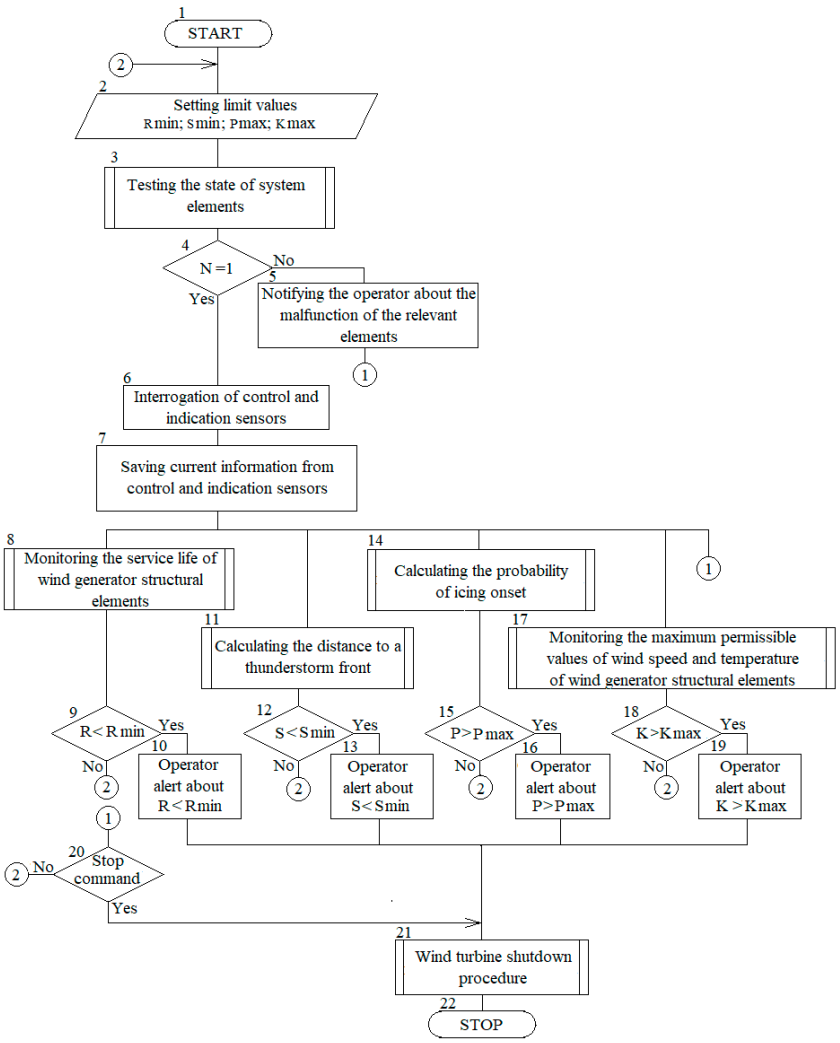


Figure 4. Combined protection system controller algorithm.

The controller program algorithm begins with program initialization (position 1, Figure 4). The initialization command is issued after power is supplied to the controller or manually from the operator's computer keyboard. The next step is to set the maximum allowable values for the monitored parameters (position 2):

Rmin—the minimum allowable coefficient value characterizing the remaining service life of the turbine's monitored components;

Smin—the minimum allowable distance to the approaching storm front;

Pmax—the maximum allowable probability of icing onset;

Kmax—the coefficient characterizing the maximum allowable wind speed and the temperature of the turbine's structural elements.

Adjustments to the allowable values can be made after stopping the program using the "Stop" command (position 20). The next step in the algorithm is to test the operability of the system components (position 3). If all components are operational (condition N = 1, position 4), the system will proceed with polling the control and indication sensors (position 6). If any component is malfunctioning, a failure message will be generated and displayed on the operator's desktop (position 5), and the turbine will be shut down following standard procedures.

To further process the current data and determine the intensity of changes in the monitored parameters—allowing, among other things, the prediction of the remaining service life of wind turbine components—it is necessary to save the current values of the monitored coordinates (position 7).

Timely resolution of maintenance issues for the mechanical components of wind turbines reduces the risk of accidents and increases the operational profitability of the monitored assets. The calculation of the coefficient characterizing the remaining lifespan of the monitored assets (R) is performed in subroutine position 8. If the value of the remaining lifespan coefficient is less than the minimum allowable value, corresponding to the operation R < Rmin in position 9, a message indicating the need for maintenance or complete replacement of the monitored device in position 10 is generated.

If the condition R < Rmin is not met, the wind turbine is considered to be in working order, and the operation cycle proceeds. Malfunctions caused by the negative impact of lightning strikes and icing on the wind turbine have a stochastic nature.

The reduction of the probability of negative consequences from lightning strikes on the wind turbine structure is achieved through monitoring the approach of a storm front. In subroutine position 11, the current operation of calculating the distance to the storm front is implemented. If the distance to the storm front becomes less than the threshold value Smin (position 12), indicating the approach of the storm front to the wind turbine, a "Stop" command (position 20) must be generated, and the wind turbine shutdown procedure (position 21) must be executed. The shutdown procedure involves the following sequence of actions: feathering the blades to stop the wind turbine's rotation, activating the mechanical brake, disconnecting from the external power grid, and blocking the information channels of the combined protection system.

Notification of the operator about reaching the minimum distance to the thunderstorm front, Smin, is implemented in block position 13. The determination of the probability of the icing onset and its duration for the wind turbine structure is implemented in subroutine position 14. The most promising method for calculating the icing onset and duration is the development of an observer based on information channels for humidity, ambient temperature, and wind speed in the opposing direction [51]. If the probability of icing onset and duration exceeds the maximum allowable value Pmax (position 15), the operator is notified of the icing event (position 16), and the rotor shutdown procedure (position 21) is carried out.

Monitoring of the maximum allowable values for wind speed, the temperature of the transformer windings, generator windings, gearbox, and mechanical brake is implemented in subroutine position 17. If the current values of the monitored parameters exceed the maximum allowable values K > Kmax (position 18), the operator is alerted by generating the appropriate messages and recommendations (position 19) on the computer screen. The shutdown sequence is initiated in position 21, and once completed, the system reaches the "STOP" state in position 22.

3. Results

The research confirmed the effectiveness of the proposed combined protection system for wind turbines in addressing a wide range of environmental and technical challenges. These challenges, which can significantly affect the turbines' reliability and operational lifespan, were categorized into two main groups: climatic conditions and the technical condition of wind turbine components. The system was designed to monitor and mitigate the negative impact of these factors.

Impact of Climatic Factors—The system demonstrated a strong capability in predicting and responding to climatic challenges like excessive wind speeds, lightning strikes, and icing. Specifically, it achieved a 98% accuracy rate in predicting lightning strikes, thanks to the fuzzy logic-based software. In terms of icing, the system effectively forecasted both the onset and duration of icing using a three-level model that factored in wind speed, humidity,

and air temperature. This significantly reduced the risk of structural damage from ice accumulation, improving wind turbine reliability even in adverse weather.

Structural Integrity and Reliability—The combined protection system also significantly enhanced the monitoring of key mechanical and electromechanical components, such as bearings, gearboxes, and generator windings. By using real-time monitoring sensors and observer algorithms, the system accurately calculated the remaining service life of critical components. Vibration analysis and spectral characteristics helped detect early signs of wear, preventing issues that could escalate into fire hazards or mechanical breakdowns.

Prevention of Emergency Situations—The system proved highly effective in minimizing emergency situations caused by overheating, high wind loads, and lightning strikes. For example, by calculating wind speed thresholds and detecting overheating in the power transformer and gearbox, the system could preemptively shut down the turbine to avoid damage. Additionally, the real-time monitoring of wind turbine temperatures reduced the likelihood of fires.

Efficiency of Control Algorithms—The control algorithms in the protection system efficiently generated control signals in response to critical events such as incoming storms or the onset of icing. Implemented through modular controllers, these algorithms enabled quick decisions to mitigate the effects of disruptive factors. Moreover, the use of nonlinear methods to calculate derivatives of noisy signals improved the system's performance, particularly in noisy environments common to high-wind areas.

4. Discussion

An analysis of the causes leading to emergency situations in wind turbines, as well as the technical solutions for implementing protection devices, has shown that, typically, only isolated incidents have been studied, and technical solutions have been proposed to address specific emergencies. The combined protection system proposed in this paper provides comprehensive protection for wind turbines against all currently known pre-emergency and post-emergency factors. The proposed system is based on a ranked analysis of wind turbine emergencies, taking into account the existing technical solutions for converting wind energy into electrical energy. The system also considers the specific features of wind turbine operation when transmitting electricity to the grid.

The developed algorithm with parallel data processing enables the system to independently implement protection for any monitored parameter in real time. Since the maximum allowable values of controlled parameters can vary in different regions of the world where wind turbines are operated, the algorithm allows for adjustments accordingly.

5. Conclusions

This paper establishes the importance of developing a combined protection system for wind turbines and includes an analysis of wind turbine designs. A structural diagram of the hardware and software components and an algorithm for the control controller of the combined protection system have been developed. The paper also analyzes disruptive factors caused by environmental conditions and the technical state of wind turbine components.

The development of the combined protection system is based on well-known scientific studies and technical solutions for individual protection components of wind turbines, which are reviewed in this paper.

The proposed combined protection system ensures the real-time monitoring of environmental parameters and maintains the technical condition of wind turbine components. The system provides protection against wind speed excesses, lightning strikes, and icing, as well as monitors the lifespan and temperature of wind turbine components.

A future direction for the development of the combined wind turbine protection system is the creation of algorithms for monitoring icing and the approach of storm fronts.

Author Contributions: Conceptualization, S.I., V.K. and G.N.; methodology, S.I. and G.T.; software, A.M.; validation, V.K.; formal analysis, S.I. and G.T.; investigation, G.E. and A.M.; resources, S.I.; data curation, G.T.; writing—original draft preparation, S.I. and V.K.; writing—review and editing, S.I. and A.M.; visualization, G.E.; supervision, S.I.; project administration, S.I.; funding acquisition, S.I. All authors have read and agreed to the published version of the manuscript.

Funding: Participation in the research of the authors V.K., G.N., G.E., S.I. and A.M. was funded of the Science Committee of the Ministry of Science and Higher Education of the Republic of Kazakhstan within the framework of the grant "Development of indirect thermal protection systems for asynchronous generators of wind power plants" (Grant No. AP19677354, 2024).

Data Availability Statement: The original contributions presented in the study are included in the article, further inquiries can be directed to the corresponding authors.

Acknowledgments: The authors acknowledge the use of ChatGPT, an AI language model developed by OpenAI, for language editing purposes. The tool was employed solely to enhance the clarity of the English text, and it did not contribute to the generation, analysis, or interpretation of the scientific content.

Conflicts of Interest: The authors declare no conflicts of interest.

References

1. European Parliament and Council. Decision (EU) 2022/591 on a General Union Environment Action Program to 2030. 2022. Available online: http://data.europa.eu/eli/dec/2022/591/oj (accessed on 8 October 2024).
2. U.S. Energy Information Administration. *Monthly Energy Review: December 2023*; U.S. Energy Information Administration: Washington, DC, USA, 2023; p. 296.
3. Healy, L. *2022 Snapshot: Clean Energy Australia Report*; Tilt Renewables: Rye Park, Australia, 2023; pp. 11–15.
4. Chien, F.; Hsu, C.-C.; Ozturk, I.; Sharif, A.; Sadiq, M. The role of renewable energy and urbanization towards greenhouse gas emission in top Asian countries: Evidence from advance panel estimations. *Renew. Energy* **2022**, *186*, 207–216. [CrossRef]
5. Enevoldsen, P.; Permien, F.-H.; von Krauland, A.-K. Corrigendum to "How much wind power potential does Europe have? Examining European wind power potential with an enhanced socio-technical atlas". *Energy Policy* **2019**, *132*, 1092–1100. [CrossRef]
6. Hoen, B.; Firestone, J.; Rand, J.; Elliot, D.; Hübner, G.; Pohl, J.; Wiser, R.; Lantz, E.; Haac, T.R.; Kaliski, K. Attitudes of U.S. wind turbine neighbors: Analysis of a nationwide survey. *Energy Policy* **2019**, *134*, 110981. [CrossRef]
7. Bórawski, P.; Bełdycka-Bórawska, A.; Jankowski, K.J.; Dubis, B.; Dunn, J.W. Development of wind energy market in the European Union. *Renew. Energy* **2020**, *161*, 691–700. [CrossRef]
8. Williams, E.; Hittinger, E.; Carvalhoa, R.; Williams, R. Wind power costs expected to decrease due to technological progress. *Energy Policy* **2017**, *106*, 427–435. [CrossRef]
9. Noel, W.; Mapping, T.M.; Yu, Q.; Leach, A.; Brian, A. Mapping the evolution of Canada's wind energy fleet. *Energy* **2022**, *167*, 112690. [CrossRef]
10. Yang, N.; Yang, J.; Pang, M.; Zhang, P.; Chang, Y.; Zhang, L.; Hao, Y.; Chen, Y. Decarbonization of the wind power sector in China: Evolving trend and driving factors. *Environ. Impact Assess. Rev.* **2023**, *103*, 107292. [CrossRef]
11. Maia, N.Z.; Almeida, L.P.; Nicolodi, J.L.; Calliari, L.; Castelle, B. Long-Term trends and wave climate variability in the South Atlantic Ocean: The influence of climate indices. *Reg. Stud. Mar. Sci.* **2023**, *66*, 103131. [CrossRef]
12. Asadi, M.; Ramezanzade, M.; Pourhossein, K. A global evaluation model applied to wind power plant site selection. *Appl. Energy* **2023**, *336*, 120840. [CrossRef]
13. Asadi, M.; Nikolopoulos, E.; Magnusson, L.; Tewari, M.; Wang, Z.; Chen, D.; Van Doan, Q.; Kusaka, H.; Ramamurthy, P.; Ray, P.; et al. Overview of extreme weather events, impacts, and forecasting techniques. In *Extreme Weather Forecasting*; Elsevier: Amsterdam, The Netherlands, 2023; pp. 1–86.
14. Hopwood, D. Generation innovation: Part two: We continue our focus on cost reduction in wind energy, and ask some major innovators in the sector where we are heading for in the major markets. *Renew. Energy Focus* **2011**, *12*, 36–41. [CrossRef]
15. Gao, Q.; Hayward, J.A.; Sergiienko, N.; Khan, S.S.; Hemer, M.; Ertugrul, N.; Ding, B. Detailed mapping of technical capacities and economics potential of offshore wind energy: A case study in South-eastern Australia. *Renew. Sustain. Energy Rev.* **2024**, *189 Part A*, 113872. [CrossRef]
16. Ullah, T.; Sobczak, K.; Liśkiewicz, G.; Khan, A. Two-Dimensional URANS Numerical Investigation of Critical Parameters on a Pitch Oscillating VAWT Airfoil under Dynamic Stall. *Energies* **2022**, *15*, 5625. [CrossRef]
17. Siemens Gamesa Renewable Energy. *Unmatched in the U.S.: Siemens Gamesa SG 14-222 DD Offshore Wind Turbines to Power 2.6-GW Dominion Energy Project*; Siemens Gamesa Renewable Energy: Hamburg, Germany, 2020; p. 3.
18. Vestas-American Wind Technology. *Vestas Is Readying New York for Offshore Wind and Moves forward Conditional Agreement for the Empire Wind 1 Project*; Vestas-American Wind Technology: Portland, OR, USA, 2024.

19. Syuhada, A.; Sary, R.; Afandi, D.; Fahriza, I. Study of blades number influence on the rotation of the turbine shaft on a horizontal axis wind turbine. In Proceedings of the 4th International Conference on Experimental and Computational Mechanics in Engineering, Banda Aceh, Indonesia, 14 September 2022; Lecture Notes in Mechanical Engineering; Springer: Singapore, 2022; pp. 473–481.
20. Monjardín-Gámez, J.J.; Campos-Amezcua, R.; Gómez-Martínez, R. Large eddy simulation and experimental study of the turbulence on wind turbines. *Energy* **2023**, *273*, 127234. [CrossRef]
21. Solodusha, S.; Suslov, K. An approach to stabilizing the dynamic loads of a wind turbine generator based on the control of the blades setting angle. *IFAC-PapersOnLine* **2022**, *55*, 76–80. [CrossRef]
22. SeaTwirl. S2x from SeaTwirl: Wind Power Engineering of the Next Generation. 2024. Available online: https://seatwirl.com/products/ (accessed on 10 October 2024).
23. Lu, W.; Roberts, A.U.S. Patent and Trademark Office. U.S. Patent No. 8067878 B1, 29 November 2011.
24. Ferguson, F.D.U.S. Patent and Trademark Office. U.S. Patent No. 7335000 B2, 19 February 2008.
25. Yagi, T.; Tojyo, T.; Makino, H.U.S. Patent and Trademark Office. U.S. Patent No. 8929049 B2, 6 January 2015.
26. Hao, Y.; Hu, L.; Zhaohao, D.; Cheng, L. Two-Stage optimal configuration of condenser for high-proportion wind power sending-end power grid considering short circuit ratio increase and transient overvoltage suppression. *Dianwang Jishu Power Syst. Technol.* **2024**, *48*, 540–551.
27. Wei, Y.; Peng, K.; Ma, Y.; Sun, Y.; Zhao, D.; Ren, X.; Yang, S.; Ahmad, M.; Pan, X.; Wang, Z.; et al. Validation of ERA5 boundary layer meteorological variables by remote-sensing measurements in the Southeast China mountains. *Remote Sens.* **2024**, *16*, 548. [CrossRef]
28. Lane, T.P.; King, A.D.; Perkins-Kirkpatrick, S.; Pitman, A.; Alexander, L.; Arblaster, J.; Bindoff, N.; Bishop, C.; Black, M.; Bradstock, R.; et al. Attribution of extreme events to climate change in the Australian region: A review. *Weather Clim. Extrem.* **2023**, *42*, 100622. [CrossRef]
29. Luchetti, N.T.; Friedrich, K.; Rodell, C.E.; Lundquist, J.K. Characterizing thunderstorm gust fronts near complex terrain. *J. Appl. Meteorol. Climatol.* **2020**, *148*, 3267–3286. [CrossRef]
30. Arrieta-Prieto, M.; Schell, K.R. Spatially transferable machine learning wind power prediction models: V-Logit random forests. *Renew. Energy* **2024**, *223*, 120066. [CrossRef]
31. Wang, J.; Chen, L.; Li, S. Characteristics of spring Mongolian cyclones in the recent 70 years: Background circulations and weather influences. *Int. J. Climatol.* **2024**, *44*, 328–343. [CrossRef]
32. Yunpeng, L.; Yunhai, L.; Meng, L. Typhoon Chan-Hom induced sediment cross-shore transport in the mud depo-center of the East China Sea inner shelf. *Mar. Geol.* **2015**, *469*, 107223.
33. Andrews, M.S.; Gensini, V.A.; Haberlie, A.M.; Ashley, W.S.; Michaelis, A.C.; Taszarek, M. Climatology of the elevated mixed layer over the contiguous United States and Northern Mexico using ERA5: 1979–2021. *J. Clim.* **2024**, *37*, 1833–1851. [CrossRef]
34. Baggett, C.F.; Nardi, K.M.; Childs, S.J.; Zito, S.N.; Barnes, E.A.; Maloney, E.D. Skillful subseasonal forecasts of weekly tornado and hail activity using the Madden-Julian Oscillation. *J. Geophys. Res. Atmos.* **2018**, *123*, 12661–12675. [CrossRef]
35. Veloso-Aguila, D.; Rasmussen, K.L.; Maloney, E.D. Tornadoes in Southeast South America: Mesoscale to planetary-scale environments. *Mon. Weather Rev.* **2024**, *152*, 295–318. [CrossRef]
36. Yushu, R.; Weixin, X.; Jiaolan, F. Characteristics of intracloud lightning to cloud-to-ground lightning ratio in thunderstorms over Eastern and Southern China. *Atmos. Res.* **2024**, *300*, 107231.
37. Campos, C.; Couto, F.T.; Santos, F.L.M.; Rio, J.; Ferreira, T.; Salgado, R. ECMWF lightning forecast in mainland Portugal during four fire seasons. *Atmosphere* **2024**, *15*, 156. [CrossRef]
38. Ul, A.N.; Farhan, M.; Chong, T. Lightning nowcasting using fuzzy logic—A risk assessment framework for resilience of microgrids. *Electr. Power Syst. Res.* **2024**, *230*, 110253.
39. Laiz, S.; Neal, R.; Pope, J.O. Identification of weather patterns and transitions likely to cause power outages in the United Kingdom. *Commun. Earth Environ.* **2024**, *5*, 49.
40. Cavaiola, M.; Cassola, F.; Sacchetti, D.; Ferrari, F.; Mazzino, A. Hybrid AI-enhanced lightning flash prediction in the medium-range forecast horizon. *Nat. Commun.* **2024**, *15*, 1188. [CrossRef]
41. Błęcki, J.; Iwański, R.; Wronowski, R.; Jujeczko, P. Study of the lightning activity over Poland for different solar activity. *Artif. Satell.* **2022**, *57*, 194–209. [CrossRef]
42. Li, C.; Hu, Q.; Wang, J.; Li, J.; Zhou, M.; Li, Q.; Fan, Y. Characterization of close electric field waveforms from triggered lightning. *IEEE Trans. Electromagn. Compat.* **2021**, *63*, 2033–2040.
43. Hong, H.; Wang, B.; Lu, G.; Li, X.; Ge, Q.; Xie, A.; Wu, Y.; Qiu, X.; Chen, J. Tracking lightning through 3D thunder source location with distributed acoustic sensing. *J. Geophys. Res. Atmos.* **2024**, *129*, e2023JD038882. [CrossRef]
44. Arechiga, R.O.; Johnson, J.B.; Edens, H.E.; Thomas, R.J.; Rison, W. Acoustic localization of triggered lightning. *J. Geophys. Res. Atmos.* **2011**, *116*, D09103. [CrossRef]
45. Bestard, D.; Coulouvrat, F.; Farges, T. Localization and quantification of the acoustical power of lightning flashes. In Proceedings of the Forum Acusticum 2023: 10th Convention of the European Acoustics Association, Torino, Italy, 11–15 September 2023.
46. Lakhdar, A. Numerical simulation of the negative downward leader current with the associated Far-EM field generated by lightning. *IEEE Trans. Electromagn. Compat.* **2024**, *66*, 240–246. [CrossRef]

47. Rotondo, D.; Cristofaro, A.; Johansen, T.A.; Nejjari, F.; Puig, V. Robust fault and icing diagnosis in unmanned aerial vehicles using LPV interval observers. *Int. J. Robust Nonlinear Control* **2024**, *29*, 5456–5480. [CrossRef]
48. Rotondo, D.; Cristofaro, A.; Johansen, T.A.; Nejjari, F.; Puig, V. Diagnosis of icing and actuator faults in UAVs using LPV unknown input observers. *J. Intell. Robot. Syst. Theory Appl.* **2018**, *91*, 651–665. [CrossRef]
49. Corradini, M.L.; Ippoliti, G.; Orlando, G. A sliding mode observer-based icing detection and estimation scheme for wind turbines. *J. Dyn. Syst. Meas. Control Trans. ASME* **2018**, *140*, 014502. [CrossRef]
50. Corradini, M.L.; Ippoliti, G.; Orlando, G. A robust observer for detection and estimation of icing in wind turbines. In Proceedings of the IECON (Industrial Electronics Conference), Florence, Italy, 24–27 October 2016; pp. 1894–1899.
51. Ying, L.; Xu, Z.; Zhang, H.; Xu, J.; Cheng, X. Graph temporal attention network for imbalanced wind turbine blade icing prediction. *IEEE Sens. J.* **2024**, *24*, 9187–9196. [CrossRef]
52. Huang, X.; Wang, Y.; Zhu, Y. Icing forecast of transmission line based on genetic algorithm and fuzzy logic. *Gaodianya Jishu/High Volt. Eng.* **2016**, *42*, 1228–1235.
53. Li, Q.; Gou, Y.; Liu, S.; Rao, Y. A detection method of ice accretion based on flash pulse infrared thermography. *Trans. Nanjing Univ. Aeronaut. Astronaut.* **2023**, *40*, 105–111.
54. Qu, J.; Wang, Q.; Peng, B.; Yi, X. Icing prediction method for arbitrary symmetric airfoil using multimodal fusion. *Hangkong Dongli Xuebao/J. Aerosp. Power* **2024**, *39*, 20220143.
55. Wang, L.; He, Y.; He, Y. Wind turbine blade icing risk assessment considering power output predictions based on SCSO-IFCM clustering algorithm. *Renew. Energy* **2024**, *223*, 119969. [CrossRef]
56. Yu, S.; Song, M.; Gao, R. A review of icing prediction techniques for four typical surfaces in low-temperature natural environments. *Appl. Therm. Eng.* **2024**, *241*, 122418.
57. Zhuang, C.; Zhang, Y.; You, F.; Cheng, Z.; Lin, G. Thermal aging analyses of a gearbox oil used for wind turbine nacelles. *J. Phys. Conf. Ser.* **2022**, *2166*, 012047. [CrossRef]
58. Zhang, Y.; You, F.; Sun, W.; Li, P.; Lin, W.; Shu, C. Fire hazard analyses of typical oils in wind turbine nacelle based on single and composite indices. In Proceedings of the 9th International Conference on Fire Science and Fire Protection Engineering (ICFSFPE 2019), Chengdu, China, 18–20 October 2019; p. 9055848.
59. Kramti, S.E.; Ali, J.B.; Bechhoefer, E.; Takrouni, K.; Darghouthi, A.; Sayadi, M. Toward an online strategy for mechanical failures diagnostics inside wind turbine generators based on spectral analysis. *Wind Eng.* **2021**, *45*, 782–792. [CrossRef]
60. Sai Balaji, M.A.; Katiyar, J.K.; Eakambaram, A.; Sethupathi, B.P.; Kamalakannan, J.; Baskar, A. Comparative study of sintered and composite brake pad for wind turbine applications. *Proc. Inst. Mech. Eng. Part J J. Eng. Tribol.* **2023**, *237*, 1430–1445. [CrossRef]
61. Xiong, G.; Zhang, Y.; Yang, P.; Zhu, Z.; Hu, P. An analysis of the burning accident of the tower bottom cabinet of G58-850KW wind turbine group. *IOP Conf. Ser. Earth Environ. Sci.* **2020**, *508*, 012054. [CrossRef]
62. Liu, X.; Bai, Y.; Wang, X.; Ding, X.; Zhang, J.; Zhang, T.; Zhang, K. Evaluation method of insulation system for wind turbine generator based on accelerated multi-factor ageing test. In Proceedings of the Annual Report—Conference on Electrical Insulation and Dielectric Phenomena (CEIDP), Shenzhen, China, 20–23 October 2013; pp. 56–59.
63. Liu, X.; Zhang, T.; Bai, Y.; Ding, X.; Wang, Y. Effects of accelerated repetitive impulse voltage aging on performance of model stator insulation of wind turbine generator. *IEEE Trans. Dielectr. Electr. Insul.* **2014**, *21*, 1606–1615. [CrossRef]
64. Arabul, A.Y.; Arabul, F.K.; Jayaram, S.H. Investigation of temperature effects on the ageing of paper oil insulation under repetitive transient voltages. In Proceedings of the 2023 IEEE Electrical Insulation Conference (EIC), Quebec City, QC, Canada, 18–21 June 2023.
65. Caponetti, F.; Kjær, M.A. Control of Wind Turbines. China Patent No. CN104937263A, 14 April 2017.
66. Hu, S.; Xie, C.; Yin, C. An adaptive reclosing scheme for cross-line faults on double-circuit wind power outgoing lines with shunt reactors. *Energies* **2024**, *17*, 1273. [CrossRef]
67. Satya Bharath, K.V.; Haque, A.; Khan, M.A.; Kuma, R. Failure mode effect classification for power electronics converters operating in a grid-connected system. *IEEE Syst. J.* **2023**, *17*, 3138–3149.
68. Simonov, A.; Ilyushin, P.; Suslov, K. On the prevention of voltage resonance at the point of wind farm connection to the distribution network. In Proceedings of the 2023 IEEE International Conference on Electrical, Computer and Energy Technologies (ICECET), Cape Town, South Africa, 16–17 November 2023.
69. Torkzadeh, R.; van Waes, J.; Ćuk, V.; Cobben, S. Model validation for voltage dip assessment in future networks. *Electr. Power Syst. Res.* **2023**, *217*, 109099. [CrossRef]
70. Lebsir, A.; Bentounsi, A.; Benbouzid, M.E.H. Electric generators fitted to wind turbine systems: An up-to-date comparative study. *J. Electr. Syst.* **2015**, *11*, 281–295.
71. Mohanrajan, S.R.; Krishna, S.V.; Reddy, L.N.; Teja, A.S.; Vishal, B. A study of motor-generator topologies for pumped storage applications. In Proceedings of the Conference on Advances in Engineering and Technology (ICAET 2014), Chandigarh, India, 7–8 February 2014; pp. 627–635. [CrossRef]
72. Enany, T.A.; Mostafa, M.A.; Othman, E.S. Direct current signal injection enhanced with artificial intelligence technique for asynchronous motors thermal monitoring. In Proceedings of the Twentieth International Middle East Power Systems Conference (MEPCON), Cairo, Egypt, 18–20 December 2018; pp. 828–833. [CrossRef]
73. Xi'an Huaao. Motor Overheating Protection Relay. China Patent No. CN102487191A, 13 June 2012.
74. Fish, M.W.; Alexander, D.F. Thermal Motor Protector. U.S. Patent US2463935A, 1 March 1949.

75. Anderson, C. *Wind Turbines: Theory and Practice*; Cambridge University Press: Cambridge, UK, 2020.
76. Toma, C. Fn extension of the notion of observability at filtering and sampling devices. In Proceedings of the International Symposium on Signals, Circuits and Systems (Iasi SCS), Sydney, Australia, 6–9 May 2001; pp. 233–236.
77. Li, H.; Gedikli, E.D.; Lubbad, R. Exploring time-delay-based numerical differentiation using principal component analysis. *Phys. A* **2020**, *556*, 124839. [CrossRef]

Disclaimer/Publisher's Note: The statements, opinions and data contained in all publications are solely those of the individual author(s) and contributor(s) and not of MDPI and/or the editor(s). MDPI and/or the editor(s) disclaim responsibility for any injury to people or property resulting from any ideas, methods, instructions or products referred to in the content.